

## Multiwavelength campaign on Mrk 509. Testing realistic Comptonization models.

**P.O. Petrucci<sup>\*†</sup>, S. Paltani<sup>1</sup>, J. Malzac<sup>2</sup>, J. Kaastra<sup>3</sup>, M. Cappi<sup>4</sup>, G. Ponti<sup>5</sup>, B. de Marco<sup>6</sup>, G. Kriss<sup>7</sup>, K. Steenbrugge<sup>8</sup>, S. Bianchi<sup>9</sup>, G. Branduardi-Raymont<sup>10</sup>, M. Mehdipour<sup>10</sup>, E. Costantini<sup>3</sup>, M. Dadina<sup>4</sup>, P. Lubiński<sup>11</sup>**

*\*UJF-Grenoble 1 / CNRS-INSU, Institut de Planétologie et d'Astrophysique de Grenoble (IPAG) UMR 5274, Grenoble, France, <sup>1</sup>ISDC, Astronomical Observatory of the University of Geneva Versoix, Switzerland, <sup>2</sup>Université de Toulouse, UPS-OMP, IRAP, Toulouse, France, <sup>3</sup>SRON Netherlands Institute for Space Research, Utrecht, the Netherlands, <sup>4</sup>INAF-IASF Bologna, Italy, <sup>5</sup>School of Physics and Astronomy, University of Southampton, Southampton UK, <sup>6</sup>Centro de Astrobiología (CSIC-INTA), Dep. de Astrofísica; LAEFF, Madrid, Spain, <sup>7</sup>Space Telescope Science Institute, Baltimore, MD 21218, USA, <sup>8</sup>Instituto de Astronomía, Universidad Católica del Norte, Antofagasta, Chile, <sup>9</sup>Dipartimento di Fisica, Università degli Studi Roma Tre, Roma, Italy, <sup>10</sup>Mullard Space Science Laboratory, University College London, Holmbury St. Mary, UK, <sup>11</sup>Centrum Astronomiczne im. M. Kopernika, Toruń, Poland*

Mrk 509 was observed by *XMM-Newton* and *INTEGRAL* in October/November 2009, with one observation every four days for a total of ten observations. Each observation has been fitted with a realistic thermal Comptonization model for the continuum emission. Prompted by the correlation between the UV and soft X-ray flux, we used a thermal Comptonization component for the soft X-ray excess. The UV to X-ray/gamma-ray emission of Mrk 509 can be well fitted by these components, pointing to the existence of a hot ( $kT \sim 100$  keV), optically-thin ( $\tau \sim 0.5$ ) corona producing the primary continuum. In contrast, the soft X-ray component requires a warm ( $kT \sim 1$  keV), optically-thick ( $\tau \sim 10$ -20) plasma. Estimates of the amplification ratio for this warm plasma support a configuration relatively close to the “theoretical” configuration of a slab corona above a passive disk. This plasma could be the warm upper layer of the accretion disk. In contrast, the hot corona has a more photon-starved geometry. The high temperature ( $\sim 100$  eV) of the soft-photon field entering and cooling it favors a localization of the hot corona in the inner flow. This soft-photon field could be part of the comptonized emission produced by the warm plasma.

*An INTEGRAL view of the high-energy sky (the first 10 years)“ 9th INTEGRAL Workshop and celebration of the 10th anniversary of the launch, October 15-19, 2012  
Bibliothèque Nationale de France, Paris, France*

<sup>\*</sup>Speaker.

<sup>†</sup>pierre-olivier.petrucci@obs.ujf-grenoble.fr

## 1. The data

Mrk 509 is a Seyfert 1 galaxy that harbors a super massive black hole of  $1.4 \times 10^8$  solar masses [6]. It was the object of an intense optical/UV/X-rays/gamma-rays campaign in late 2009, with the participation of five satellites (*XMM-Newton*, INTEGRAL, Swift, Chandra, and HST) and ground-based telescopes (WHT and PAIRITEL). The source characteristics and the whole campaign are explained in [3]. The main objective of this campaign was to study in detail the physical properties and structure of the warm-absorber outflows in Mrk 509. The heart of the monitoring are ten simultaneous *XMM-Newton*/INTEGRAL observations, with one observation every four days (60 ks with *XMM-Newton* and 120 ks with INTEGRAL). We have tested these simultaneous UV to X-rays/gamma rays data against physically motivated broad band models [8].

## 2. Model-independent results

### 2.1 Correlations

An important result observed during this campaign is the strong correlation between the UV and soft X-ray ( $<0.5$  keV) flux, while no correlation was found between the UV and the hard ( $>3$  keV) X-rays (see [4] and Fig. 1a). This suggests that the UV and soft X-ray excess variability observed on the timescale of the campaign is produced by the same spectral component, possibly thermal Comptonization.

### 2.2 Principal component analysis

We perform a principal component analysis (PCA) to search for variability patterns. The first PCA components are those that reproduce most of the observed variability, with the others dominated by the statistical noise in the data. We have plotted the two first principal components of our analysis in Fig. 1b. The first component consists mainly in a variability mode dominated by flux variations in the hard energy range ( $> 1$  keV). Most of the sample variance ( $>87\%$ ) is produced by this component. The second PCA component is dominated by variability below 1 keV, and represents 10% of the total variance. The 4% of variance left is distributed between the higher order components not shown here. This result nicely supports the idea that two main components are dominating the broad-band variability of this campaign, one in the UV-soft X-rays and the other in the hard X-rays.

## 3. Spectral analysis

The purpose of the present paper is not to test different models (especially concerning the soft X-ray excess or the primary continuum). We instead make the choice of fitting a few, physically motivated spectral components, which will permit us to discuss the corresponding physical interpretation of the data in depth.

### 3.1 The model components

**The warm absorber:** the WA has been comprehensively analyzed by [1], and we refer the reader to this article for more details. We produced a table from the best model of the WA derived from this analysis and included this table in XSPEC.

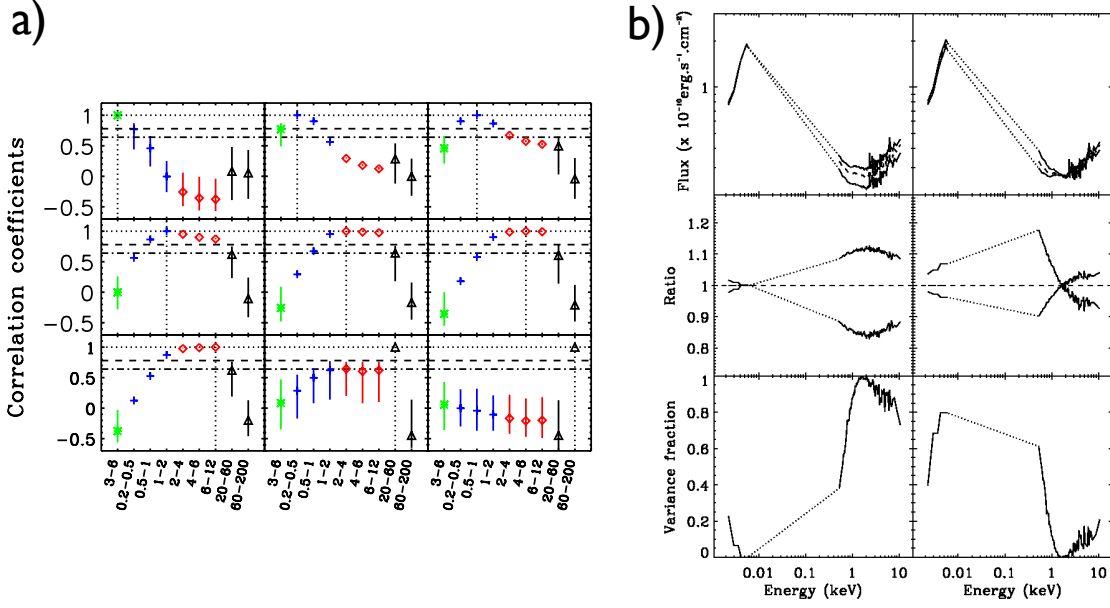


**Figure 1:** **a)** Count rate-count rate correlation coefficients between different energy bands for the 10 observations. In each panel, the light curves are correlated with the one marked with the vertical dotted lines. We have overplotted the 95% and 99% confidence levels for the significance of the correlation with horizontal dot-dashed and dashed lines, respectively. **b)** The two principal mode of variability. The upper panels show the time average spectrum (dashed line) and the spectra corresponding to the extrema of the first (left) and second (right) variability mode. The middle panels show the ratio of the maximum and minimum spectra to the total spectrum of the source. The bottom panels show the contribution of each component to the total variance as a function of energy.

**The soft X-ray excess:** Following [4], we chose to model the UV-soft X-ray emission by thermal Comptonization of what we call a WARM corona in the following. We used the NTHCOMP model of XSPEC. The free parameters of NTHCOMP are the temperature of the corona  $kT_{wc}$ <sup>1</sup>, the soft-photon temperature  $T_{bb,wc}$ , and the asymptotic power-law index  $\Gamma_{wc}$  of the spectrum. Note however that NTHCOMP does not provide the corona optical depth directly. It has to be deduced in another manner, generally by comparing its spectral shape to another model that provides the optical depth. This is, however, a possible source of uncertainties. In the following, the optical depth of the WARM corona is deduced from a comparison with the EQPAIR model.

**The primary continuum:** We used the Comptonization model COMPPS [10] of XSPEC to model the high-energy primary continuum. COMPPS is well adapted to reproducing the emission of a hot and optically thin plasma, i.e., what we call the HOT corona in the following. The fit parameters of COMPPS are the temperature of the corona  $kT_{hc}$ <sup>2</sup>, either the optical depth  $\tau_{hc}$  or the parameter  $y_{hc} = 4 \frac{kT_{hc}}{m_e c^2} \tau_{hc}$ , where  $y_{hc}$  is equivalent to the Compton parameter for small ( $< 1$ ) optical depths, the temperature of the soft photons produced by the cold phase  $kT_{bb,hc}$  (also assuming a multicolor-disk distribution) and the geometry of the disk-corona configuration. We prefer to use the Compton parameter instead of the optical depth in the fitting procedure to minimize the model degeneracy. Indeed, the temperature and optical depth are generally strongly correlated in the fitting procedure,

<sup>1</sup>The letters “wc” means warm corona and refer to all the parameters of the NTHCOMP model.

<sup>2</sup>The letters “hc” mean hot corona, and refer to all the parameters of the COMPPS model.

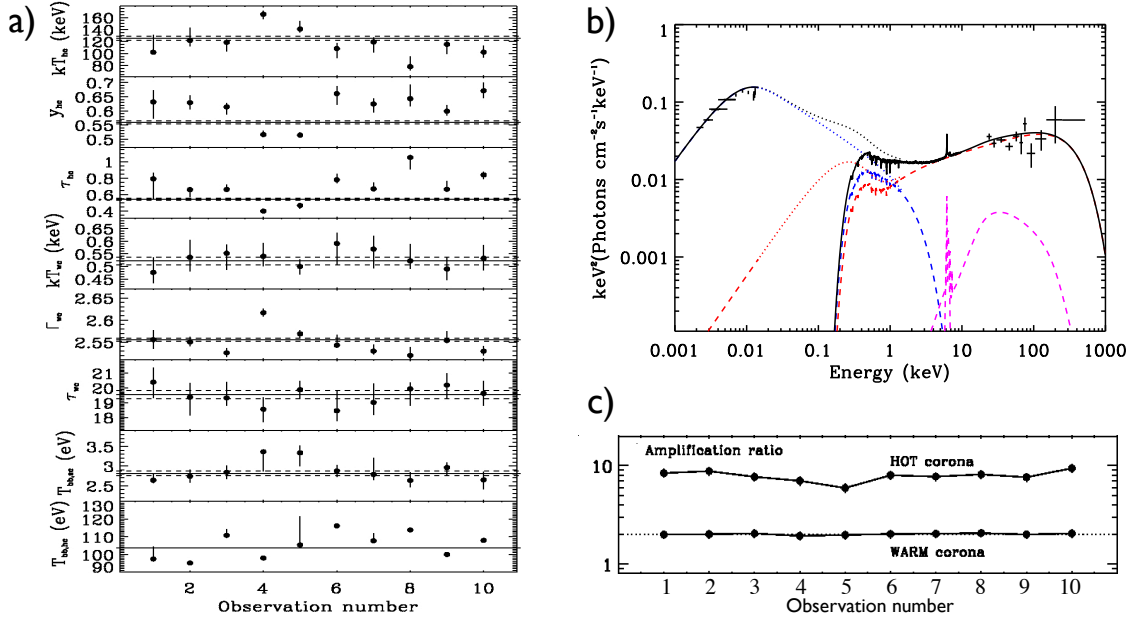


**Figure 2:** **a)** Time evolution of the different fit parameters. From top to bottom: the HOT corona temperature  $T_{hc}$ , Compton parameter  $y_{hc}$ , optical depth  $\tau_{hc}$ , and the WARM corona temperature  $T_{wc}$ , photon index  $\Gamma_{wc}$ , optical depth  $\tau_{wc}$ , and the soft photon temperatures  $T_{bb,wc}$  and  $T_{bb,hc}$ . The solid lines show the best-fit constant values and the dashed lines the  $1\sigma$  uncertainties. **b)** Unfolded best-fit model of the total data spectrum. The data are the black crosses. The solid black line is the best-fit model including all absorption (WA and Galactic). The dashed lines correspond to the different spectral components, HOT (in red) and WARM (in blue) corona emission as well as the reflection (magenta) including the effects of absorptions, while the dotted lines are absorption free. **c)** Compton amplification ratio for the WARM (bottom curve) and HOT (top curve) coroneae, respectively. The dotted line is the expected value for a thick corona in radiative equilibrium above a passive disk.

with the same 2-10 keV slope obtained with different combinations of these two parameters (e.g. [7]). We also assume a slab geometry for the corona-disk system.

**The iron line:** Following the results obtained by [9], we use PEXMON [5] to fit the narrow core of the iron line and a Gaussian to fit a broad-line component if needed.

### 3.2 Results

The two plasmas have different parameters (see light curve on Fig. 2a). The WARM corona is optically thick with  $\tau_{wc} \sim 20$ , a temperature  $kT_{wc}$  on the order of 600 eV and a soft-photon temperature  $T_{bb,wc} \sim 3$  eV. In contrast, the HOT corona is optically thin  $\tau_{hc} \sim 0.6$ , with a temperature  $kT_{hc}$  of about 100 keV and a soft-photon temperature  $T_{bb,hc} \sim 100$  eV. In this model (see Fig. 2b), the optical/UV data are entirely fitted by the low-energy part of the WARM plasma emission. The soft-photon bump of the HOT corona, instead, peaks in the soft X-ray range and contributes to the soft X-ray excess. The soft-photon temperature of  $\sim 100$  eV suggests that the HOT corona is localized in the inner region of the accretion flow compared to the WARM corona; however, a 100 eV temperature is large for a “standard” accretion disk around a  $\sim 10^8 M_{\odot}$  black hole.

We call  $L_{tot}$  the total corona luminosity and  $L_s$  the *intercepted* soft-photon luminosity, i.e., the part of the soft-photon luminosity emitted by the cold phase that effectively enters and cools the

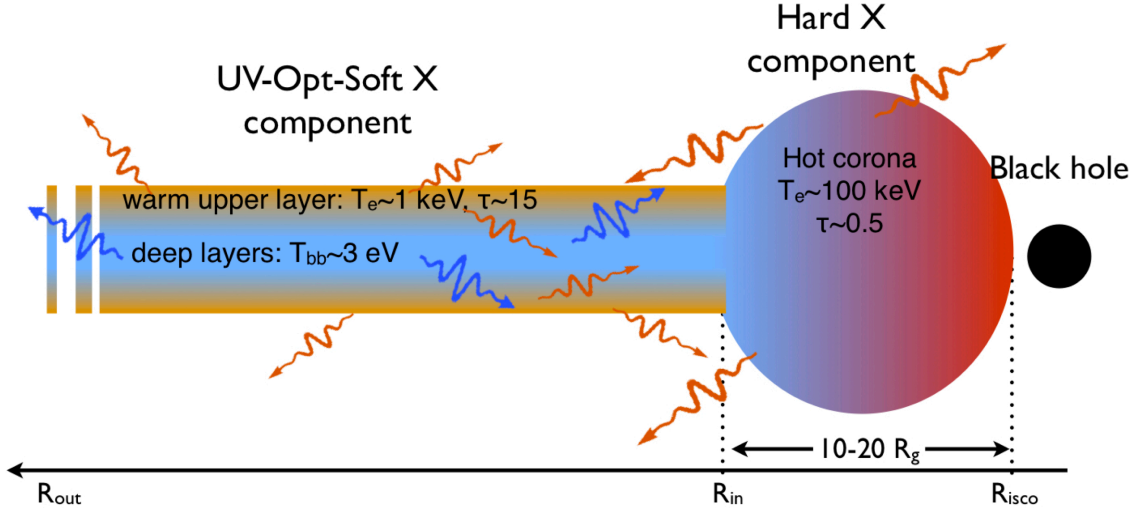


**Figure 3:** A sketch of the accretion flow geometry in the inner region of the galaxy Mrk 509. The HOT corona, producing the hard X-ray emission, has a temperature of  $\sim 100$  keV and optical depth  $\sim 0.5$ . It is localized in the inner part of the accretion flow ( $R < R_{in}$ ) and illuminates the accretion disk beyond  $R_{in}$ , helping to form a WARM layer at the disk surface. This WARM component has a temperature of  $\sim 1$  keV and an optical depth  $\sim 15$  and produces the optical-UV up to soft X-ray emission. It extends over a large part of the accretion flow, heating the deeper layers and comptonizing their optical-UV emission. In return, part of this emission enters and cools the HOT corona.

corona. The difference  $L_{tot} - L_s$  then corresponds to the intrinsic heating power provided by the corona to comptonize the seed's soft photons. The ratio  $L_{tot}/L_s$  is called the Compton amplification ratio. We have plotted the values of the amplification ratios for the ten observations, in Fig. 2c. The WARM and HOT coronae have clearly different amplification ratios. This is remarkably constant and equal to  $\sim 2$  for the WARM plasma as expected given its large optical depth (see [8]) and in between 5-15 for the HOT corona, with a significant decrease between Obs 3 and 6.

From these different results, a tentative toy picture of the overall configuration of the very inner regions of Mrk 509 could be the following (see also [2]): a HOT corona ( $T_e \sim 100$  keV,  $\tau = 0.5$ ) fills the inner part of the accretion flow, below say  $R_{in}$ . It illuminates the outer part of the disk and contributes to the formation of a warm upper layer ( $T_e \sim 1$  keV,  $\tau = 20$ ) on the disk beyond  $R_{in}$ , the WARM corona. This WARM corona also possesses its own heating process, potentially through dissipation of magnetic field at the disk surface. It heats the deeper layers of the accretion disk, which then radiates like a black body (at  $T_{bb} \sim 3$  eV). This WARM corona upscatters these optical-UV photons up to the soft X-ray, a small part of them entering and cooling the HOT corona. The small solid angle under which the hot flow sees the warm plasma agrees with the large amplification ratio of  $\sim 5-10$  estimated from our fits. The 100 eV temperature obtained by our XSPEC modeling would be explained by the fact that XSPEC would try to mimic the WARM plasma emission, which covers an energy range between  $\sim 1$  eV and  $\sim 1$  keV, with the multicolor-disk spectral energy distribution of the seed soft photons available in COMPPS. A tentative sketch is shown in Fig. 3.

#### 4. Conclusions

Mrk 509 was monitored simultaneously with *XMM-Newton* and *INTEGRAL* for one month

in late 2009, with one observation every four days for a total of ten observations. A series of papers has already been published using these data focusing on different aspects of the campaign. Here we analyzed the broad-band optical/UV/X-ray/gamma-ray continuum of the source during this monitoring. Our main effort was to adopt realistic Comptonization models to fit the primary continuum, the accretion disk, and the soft X-ray excess. We obtained a relatively good fit to the data by assuming the existence of two clearly different media: a hot ( $kT \sim 100$  keV), optically-thin ( $\tau \sim 0.5$ ) corona for the primary continuum emission, and a warm ( $kT \sim 1$  keV), optically-thick ( $\tau \sim 10$ -20) plasma for the optical-UV to soft X-ray emission.

These two media have very different geometries: the WARM corona covers a large part of the accretion disk, the disk radiation being dominated by the reprocessing of the WARM corona emission. The WARM corona could be the warm upper layer of the accretion disk. The temperature of the soft-photon field cooling it is on the order of 3 eV. In contrast, the HOT corona has a more photon-starved geometry and can be the inner part of the accretion flow. The transition radius  $R_{in}$  between the outer disk/WARM plasma and the HOT inner corona is estimated to be around 10–20  $R_g$ . The variation in  $\dot{M}$  but also in  $R_{in}$  would be at the origin of the variation in the coronae luminosities, the variation in  $R_{in}$  also producing the variation in the HOT corona amplification ratio. The spectral and flux variation in the HOT corona are also consistent with a pair-dominated plasma.

These different conclusions may depend at some level on the choice of our modelling. For example, we do not include blurred ionized reflection, while part of the soft X-ray excess could be produced by this component. On the typical time scale ( $\sim$  day) of this campaign, however, it does not seem to play a major role and Comptonization in a WARM plasma, covering the accretion disk, appears the most natural explanation for the soft X-ray excess in Mrk 509.

## References

- [1] Detmers, R. G., Kaastra, J. S., Steenbrugge, K. C., et al. 2011, *A&A*, 534, A38
- [2] Done, C., Davis, S. W., Jin, C., Blaes, O., & Ward, M. 2012, *MNRAS*, 420, 1848
- [3] Kaastra, J. S., Petrucci, P. O., Cappi, M., et al. 2011, *A&A*, 534
- [4] Mehdipour, M., Branduardi-Raymont, G., Kaastra, J. S., et al. 2011, *A&A*, 534, A39
- [5] Nandra, K., O’Neill, P. M., George, I. M., & Reeves, J. N. 2007, *MNRAS*, 382, 194
- [6] Peterson, B. M., Ferrarese, L., Gilbert, K. M., et al. 2004, *ApJ*, 613, 682
- [7] Petrucci, P. O., Haardt, F., Maraschi, L., et al. 2001, *ApJ*, 556, 716
- [8] Petrucci, P. O., Paltani, S., Malzac, J., et al. 2012, *A&A*, in press, (arXiv:1209.6438)
- [9] Ponti, G., Cappi, M., Costantini, E., et al. 2012, *A&A*, in press (<http://arxiv.org/abs/1207.0831>)
- [10] Poutanen, J. & Svensson, R. 1996, *ApJ*, 470, 249